Materials and Design 198 (2021) 109359

Contents lists available at ScienceDirect

Materials and Design

journal homepage: www.elsevier.com/locate/matdes

Solid-solution strengthening effects in binary Ni-based alloys evaluated by high-throughput calculations

Ming-Xu Wang [a], Hong Zhu [b], Gong-Ji Yang [c], Ke Liu [b], Jin-Fu Li [a], Ling-Ti Kong [a,*]

[a] School of Materials Science and Engineering, Shanghai Jiao Tong University, 800 Dongchuan Road, Minhang, Shanghai 200240, China
[b] University of Michigan—Shanghai Jiao Tong University Joint Institute, Shanghai Jiao Tong University, 800 Dongchuan Road, Shanghai 200240, China
[c] Hunan Provincial Key Laboratory of Advanced Materials for New Energy Storage and Conversion, School of Materials Science and Engineering, Hunan University of Science and Technology, Xiangtan 411201, China

HIGHLIGHTS

- Solid-solution strengthening effects of 35 elements in Ni were evaluated based on high-throughput DFT calculations.
- The strengthening ability depends on the position of the elements in the period table, and size effect dominates in general.
- Promising solutes were screened from the strengthening potential that compromises the strengthening ability and solubility.

GRAPHICAL ABSTRACT

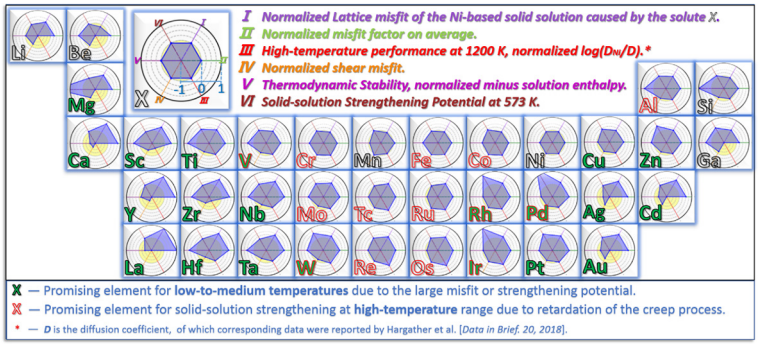

ARTICLE INFO

Article history:
Received 27 September 2020
Received in revised form 5 November 2020
Accepted 23 November 2020
Available online 27 November 2020

Keywords:
Lattice constant
Shear modulus
Misfit factor
Linear regression coefficient
First-principles calculations

ABSTRACT

Designing of new alloys requires a detailed understanding of the roles played by each alloying element, yet a systematic investigation of the solid-solution strengthening effects in Ni is still missing. High throughput density functional theory calculations were therefore performed to quantitatively assess the strengthening effects of 35 potential alloying elements from the 2nd to the 6th row of the periodic table in FCC-Ni with varying concentrations. The obtained composition-dependent lattice constants and shear moduli were employed to analyze their strengthening effects within the framework of the Labusch model. It is found that the strengthening ability correlates with the position of the element on the periodic table. Elements in both ends of each period tend to have higher strengthening abilities than those in the middle, and the lattice misfit is found to dominate the strengthening effect for elements in the 5th and 6th period. Stability analysis reveals that all the solid solution models are dynamically stable and intrinsically ductile. Thermodynamic consideration finds that roughly half of the elements are prone to form solid solutions with Ni. By adopting the experimental solubilities, the strengthening potentials of these elements were further evaluated and promising strengthening elements were screened.

1. Introduction

Ni-based singe-crystal superalloys have been widely used in aircraft and power-generation turbines, rocket engines, and other challenging environments, including nuclear power and chemical processing plants etc. in the past few decades, [1] because of their remarkable high-temperature strength, creep, fatigue, and corrosion resistances imparted by the full use of precipitation strengthening and solid-solution strengthening (SSS). It is noted that the γ′-phase precipitation strengthening has been exploited to its extreme, [2] further enhancement of the mechanical properties relies largely on exploiting the SSS

* Corresponding author.
E-mail address: konglt@sjtu.edu.cn (L.-T. Kong).

https://doi.org/10.1016/j.matdes.2020.109359

of the γ-phase. To this end, more than 10 kinds of alloying elements have been added in the state-of-the-art Ni-based singe-crystal superalloys as solutes, making it rather challenging to isolate the specific strengthening effect of each alloying element. Among them Re is known to be critical for the high-temperature performance, yet its low abundance on earth drives the need to seek for replacing elements with comparable effects. Consequently, a complete understanding of the SSS effect of the alloying elements in Ni is crucial to improve the performance of superalloys or to develop new superalloys. [3]

Great efforts and achievements have been made to understand and to quantify the SSS effect of the solute atoms. It has been revealed that the hardening is mainly caused by hindering dislocation motion due to the lattice misfit and modulus misfit between the solute and the matrix [4–6]. In the strong-pinning model proposed by Friedel [7] and Fleischer [8,9], the solute atoms in the glide plane are considered as independent point obstacles pinning the dislocations. While in the weak-pinning model presented by Labusch [10–12], the statistical distribution of the solute is considered besides the effect of temperature. It turns out that the former applies for moderately dilute alloys at 0 K, while the latter works at ambient temperatures ($T > 78$ K) for solute concentrations of relevance to engineering alloys ($c > 10^{-4}$) [3]. In recent years, some improvements [13–15] over the Labusch model have been made by incorporating the Peierls-Nabarro model, in view of the advances in computing capability that make the first-principles calculations feasible for relevant issues. All these models take necessary material parameters, such as the lattice constant, shear modulus or stacking fault energy, as inputs to make quantitative prediction of the SSS effect. These parameters, depending on the composition of the alloys in general, also affect the performance of the materials. For example, researchers [16,17] found that in moderate temperature creep the directional coarsening of the γ'-phase was sensitive to the sign and magnitude of γ/γ' lattice misfit. A detailed quantification of the composition dependence of the fundamental properties is therefore crucial for either tuning the performance of the materials or making reliable predictions of the SSS effects [18].

Some models [19–21] have been developed to describe the composition dependence of these property parameters, although they are usually of limited reliability. Among them, the Vegard's law [19] is the most well-known and widely used one that predicts the lattice parameter of a binary solid solution. However, deviation from the Vegard's law was frequently observed. Consequently, credible prediction of the SSS effect calls for reliable measurements of the composition dependent material property parameters. In this respect, experimental measurements are generally tedious and costly, while first-principles calculations based on density functional theory (DFT) are increasingly employed [22]. For instance, Wang et al. [23] studied the lattice parameters and the local lattice distortions for 11 dilute Ni-based solid solutions. Shang et al. [24] examined the temperature dependence of lattice constants and elastic constants for 26 dilute Ni-based superalloys. There are also many studies focusing on other Ni-based alloy systems [25–29]. In general, the calculated property parameters are in acceptable agreements with the available experimental data, confirming the reliability of the DFT calculations. Nonetheless, the composition dependence of the critical property parameters in Ni-based systems was barely explored. Besides, different studies frequently focused on different property parameters, while a systematic assessment of the SSS effects is still missing. A comprehensive evaluation of the SSS effect for potential alloying elements in Ni therefore awaits further systematic investigations.

The emergence of high-throughput computation makes it possible to assess the SSS effect of potential alloying elements in a consistent and efficient way. Comparing to traditional computations, it provides an automated, unified, systematical, and powerful tool for materials screening and discovery [30–32]. In this work, high-throughput DFT computations were employed to examine the composition dependences of the lattice constants, elastic constants, and energetics for the Ni-based binary solid solutions with 35 different elements from the 2nd to the 6th period of the periodic table. By combining with the Labusch model, the SSS effects of these elements in γ-Ni were quantitatively evaluated, and promising strengthening elements were identified. The findings can serve as a solid foundation and guidance for future composition design of new Ni-based superalloys.

2. Computational details

High-throughput calculations were carried out by using the ATOMATE codes as the driver to automate the workflows [33]. The equilibrium lattice constants were evaluated by adopting the preset workflow that computes and then fits the energy-volume relation of the solid solution models to the Birch-Murnaghan equation of state (EOS) [34]. The elastic constants were calculated by using the preset workflow that fits the computed energy-strain relation to polynomial functions; the average shear modulus was estimated by following the Voigt-Reuss-Hill (VRH) scheme [35].

All DFT calculations were performed by using the VASP codes [36,37], where the ion-electron interactions were described by the projector augmented wave method [38] and the GGA-PBE exchange correlation functionals [39] were employed. A plane wave cutoff energy of 520 eV was adopted with the spin polarization switched on. The electronic integration in the Brillouin zone was performed on a Γ-centered *k*-mesh with a grid density of 7000, where the partial occupations of the bands were set following the first-order Methfessel-Paxton method [40] with a smearing width of 0.05 eV. The energy tolerance for the electronic relaxations was 10^{-7} eV per atom, and the Hellmann-Feynman force tolerance for the ion relaxations was set to be 0.01 eV/Å.

A $2 \times 2 \times 2$ supercell containing 32 atoms was adopted to model the FCC-Ni based solid solution, whose cubic shape was maintained during the relaxation process while the volume was allowed to change so as to relieve the hydrostatic pressure. The random substitution was realized by following the recipes of Monte Carlo special quasi-random structure (MCSQS) [41] within the ATAT codes [42] and 4 different concentrations were considered, namely 3.125 at.% (1/32), 6.250 at.% (2/32), 9.375 at.% (3/32), and 12.500 at.% (4/32), respectively. Supercells of 108 atoms and 256 atoms were also attempted, and a supercell of 32 atoms was found to be sufficient to yield reliable results for the solid solutions.

3. Results and discussions

3.1. Composition dependence in lattice constants of Ni-X solid solutions

In the dilute limit, most properties of the solid solutions are seen to scale linearly with the solute concentration. It is therefore expected the lattice constants of the Ni-based binary substitutional solid solutions would also correlate linearly with their compositions. Indeed, a linear composition dependence was found for nearly all the alloying elements considered here. Furthermore, the linearity was seen to hold even beyond the dilute range for almost all the systems, except for elements with very low equilibrium solubility in Ni, such as La and Y, whose lattice constants showed a parabolic dependence on the composition.

The calculated lattice constants of the solid solution models for each alloying element will therefore be fitted to

$$a(c) = k_a \cdot c + a_0, \tag{1}$$

where a and a_0 are the lattice constant of the Ni-X solid solution model with a solute concentration of c and that for pure FCC-Ni, respectively. k_a is a fitting parameter, whose value reflects the size mismatch between the solute and the Ni matrix. Fig. 1(a) shows the calculated lattice constants for Ni–Al solid solutions, together with the experimental data [43,44]. One sees a perfect agreement between the experimental and calculated data. Besides, a linear composition dependence is well maintained up to the maximum solute concentration (12.500 at.%)

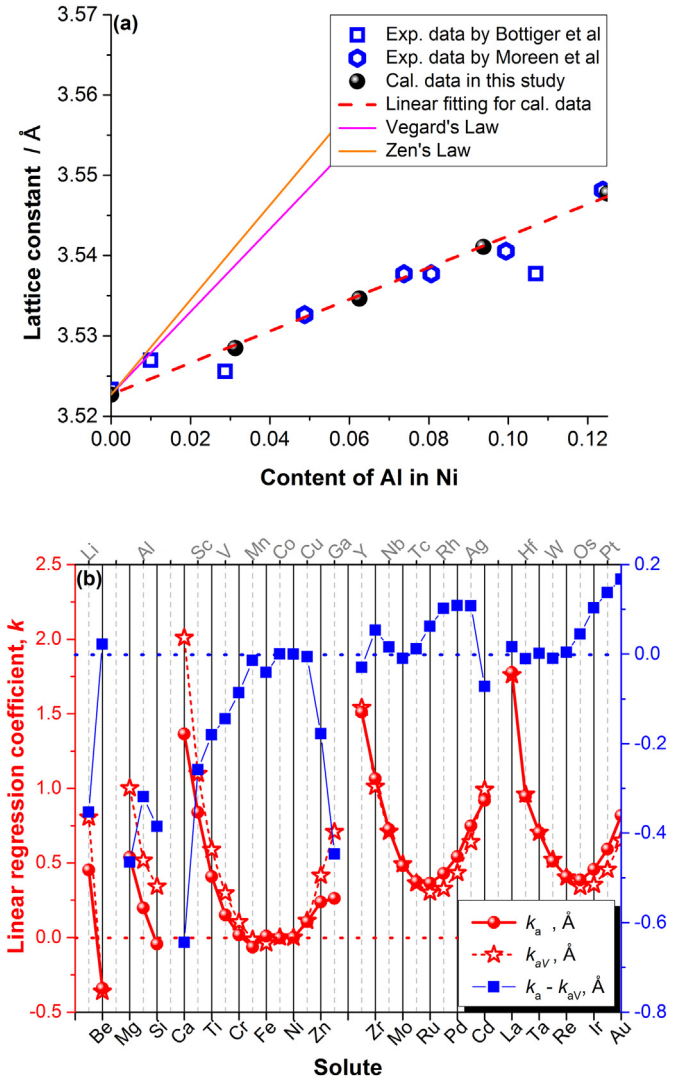

Fig. 1. (a) Lattice constants of Ni—Al solid solutions as a function of Al solute concentration, together with experimental data and predictions based on the Vegard's and the Zen's law. (b) Linear regression coefficients of the composition dependent lattice constants for Ni-based binary solid solutions with different alloying elements. Red solid circles are from the linear regression of the calculated data, and red hollow pentacles are the linear coefficient of the Vegard's law. Their differences are shown as blue solid squares.

considered here. A linear regression results in a coefficient of $k_a = 0.198$ Å and a correlation of $R^2 = 0.999$, confirming a good linearity.

The Vegard's law also predicts a linear composition dependence for the lattice constants of solid solutions. Nonetheless, the lattice constant of the solid solution is estimated by

$$a'(c) = k_{aV} \cdot c + a_0, \tag{2}$$

where $k_{aV} = a_X - a_{Ni}$, a_X is the lattice constant of element X in FCC structure. As mentioned earlier, deviation from the Vegard's law is frequently observed. The linear coefficient (k_{aV}) is determined by the lattice constants of the pure elements, instead of from fitting to the experimental/calculated data. In the case of Ni–Al, k_{aV} is found to be 0.516 Å, which is about 161% larger than k_a. In turn, one sees from Fig. 1(a) that the lattice constants predicted by the Vegard's law show large deviation from the experimental and calculated results. Incidentally, the Zen's law [45] is another model that estimates the lattice parameters of solid solutions from those of the constituting elements. Different from the Vegard's law, it adopts the composition weighted volume instead of the composition weighted lattice constant. In the case of Ni–Al, its prediction is even worse than that of the Vegard's law, and therefore no further discussion with this model will be presented.

The lattice constants for the Ni-based binary solid solution models with all the 35 alloying elements considered here were obtained from the high-throughput calculations and fitted to Eq. (1). Fig. 1(b) compiles the linear regression coefficients. It is seen that in general the variation of the linear coefficient depends on the location of the alloying element in the periodic table. Within the 4th, 5th and 6th periods, the k_a value generally shows a parabolic dependence on the atomic number of the alloying element: it firstly decreases with the increasing of the atomic number of the solute, and then increases in the end of the period. The trend correlates well with the atomic size within each group, which also decreases in the beginning and increases in the end. This should result from the well-known *d*-band filling effect of the transition metal elements. The abnormal behavior for Ni–Fe can be attributed to the complex magnetic structure. Besides, the curve for each period generally shifts upwards with the increasing period number, in line with the trend in the atomic size of the elements. One also sees that for most alloying elements, the linear coefficient is positive, suggesting that their addition to the FCC-Ni tends to dilate the lattice. Only 4 out of the 35 elements considered in this work have a negative coefficient, namely Be, Si, Mn, and Co. Nevertheless, the linear coefficients are essentially zero for Co, suggesting that their addition can hardly change the volume of FCC-Ni, in good accordance with the available reports [23,26]. More detailed information on the composition dependence in the lattice constants of these solid solutions can be found in the Supplementary file.

From Fig. 1(b) one also reads that nearly identical trends are observed for k_{aV}, except for the 3rd period. Nevertheless, the absolute values of k_a and k_{aV} differ from each other. For most elements from the 2nd to the 4th period in the periodic table, k_a is found to be smaller than k_{aV}, while for elements in the 5th and 6th period, k_a is usually larger than k_{aV}. This seems to suggest that elements in the 2nd to the 4th period tend to have strong interaction with Ni, so that alloying between them would lead to a reduction in the total volume comparing to the mechanical mixture of them. Different from the behavior of k_a or k_{aV}, the difference between them however does not show a monotonic variation against the atomic number, indicating a complicated interaction rather than merely the size effect. Many explanations have been attempted to account for the composition dependence in lattice constants in terms of size effect [46–48] and/or the electronic structure [49–51], a consistent model is however still lacking.

3.2. Composition dependence in shear modulus of Ni-X solid solutions

The full elastic tensors for the Ni-based solid solution models with different solute concentrations and alloying elements were also obtained by the high-throughput DFT calculations. For ideal FCC crystals, only three independent elastic constants are expected. The introduction of the solute however breaks the symmetry of the lattice, which will lead to unequal values for the correlated components and finite values for some components that should otherwise be zero. To overcome this, the average of correlated components was adopted for the corresponding component, and the close-to-zero finite values were ignored. For example, C_{11} takes the value of $\overline{C}_{11} = (C_{11} + C_{22} + C_{33})/3$ while C_{14} is assumed to be zero. Furthermore, since the substitutional solute atoms should distribute randomly in the substituted lattice sites, the MCSQS solid solution model actually samples one of the possible configurations. To remedy the compositional random distribution, we took the VRH average [35] shear modulus as the relevant one, which is usually employed to estimate statistically the shear modulus of a polycrystalline material from the elastic constants of its single crystal counterpart by accounting for the random distribution of the grains.

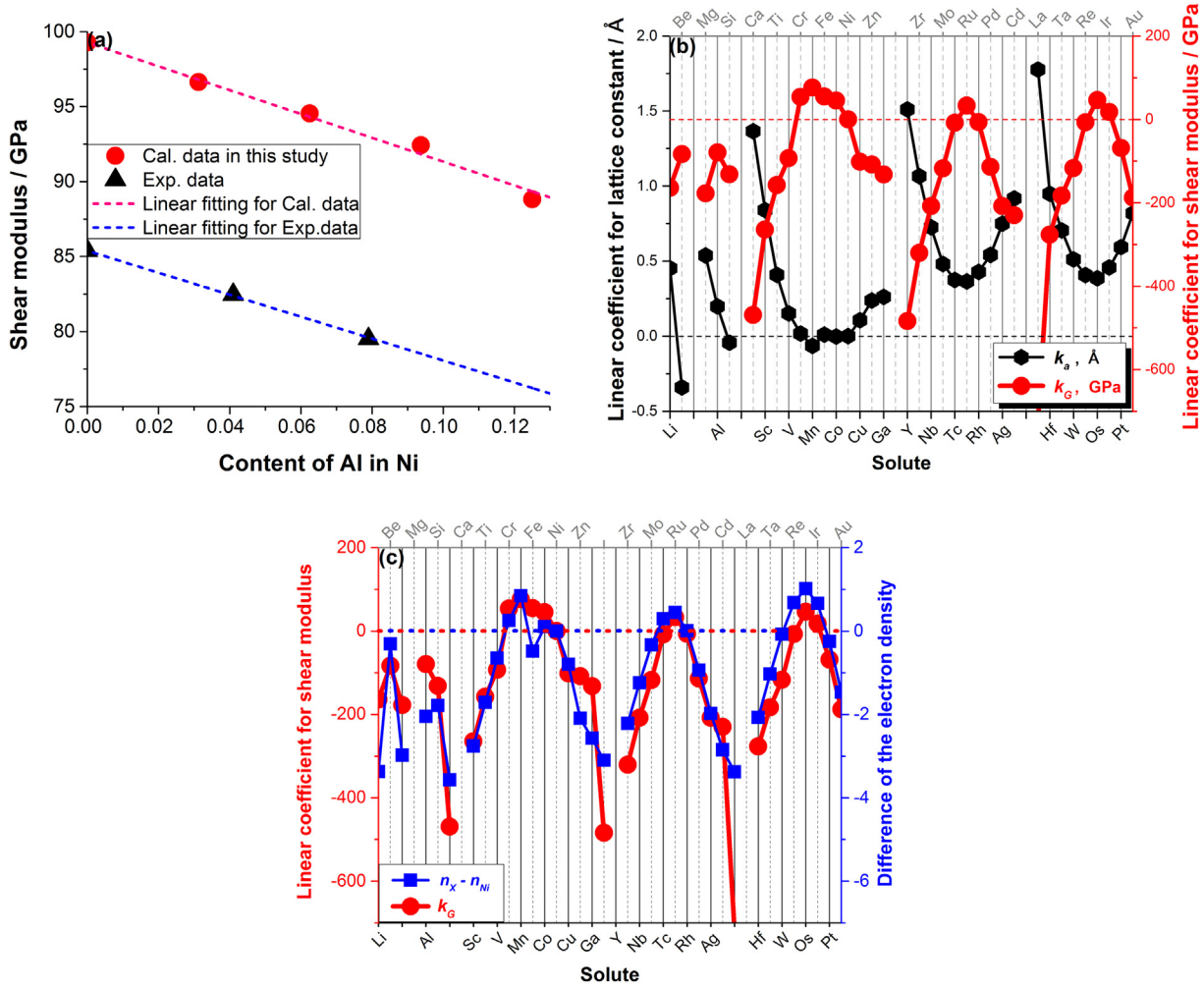

Fig. 2. (a) Shear moduli of Ni—Al solid solutions against Al solute concentration, together with the experimental data and their linear regressions. (b) Linear regression coefficients of the lattice constants and the shear moduli for Ni-based binary solid solutions. (c) Correlation between k_G and the difference in the characteristic electron density.

As an example, Fig. 2(a) shows the VRH shear modulus for Ni–Al solid solutions as a function of Al concentration. One sees that the shear modulus scales roughly linearly with the Al concentration. Consequently, we would also use linear regression to model the composition dependent shear modulus,

$$\overline{G}(c) = k_G \cdot c + \overline{G}_0, \tag{3}$$

where $\overline{G}(c)$ and $\overline{G}_0$ are the VRH shear modulus of the solid solution model $Ni_{1-c}X_c$ and FCC Ni, respectively. The linear coefficient k_G could therefore be employed to quantify the effect of alloying on the modulus misfit. Accordingly, the coefficient for the calculated shear moduli of Ni–Al solid solutions is found to be −73.2 GPa, while that for the experimental data [52] is −79.4 GPa, differing by about 8%.

Linear regression of VRH shear modulus and solute concentration data were consequently performed for all the 35 alloying elements, and Fig. 2(b) compiles the derived linear coefficients. It should be noted that for some systems, the composition dependence of shear modulus is a little bit far from linearity. Nevertheless, for most systems a linear regression provides a good approximation. One sees from Fig. 2 (b) that similar to the lattice constant case, the variations of k_G also correlates with the period number of the elements. While dissimilar to the lattice constant case, within the same period, k_G generally increases first and then decreases, showing an inverse trend as k_a. Moreover, for most alloying elements, the values of k_G are negative, indicating that most alloying elements tend to reduce the average shear modulus of the crystal. Furthermore, a positive k_a generally corresponds to a negative k_G, and vice versa. There are some exceptions, though. For instance, both k_a and k_G are positive for Fe, Ru, Os, and Ir, while both of them are negative for Be and Si. The abnormal behavior for these alloying elements deserves some extra attention.

The observed abnormal behavior in Be, Si, Ru, Os, and Ir should originate from the electronic structure. Atoms interact with each other mainly through the valence electrons, i.e., the outer core ones. For metals, the valence electrons are shared between all atoms, forming an electronic sea that glues the nuclei together. The addition of different solute atoms will introduce disturbance to the electron sea, and in turn affects the property and behavior of the solid solution. An increase in the electron density tends to enhance the metallic interatomic bonding, and hence an improved modulus. Yet the disturbance to the electron density also correlates with the volume change induced. In this regard, Miedema et al. [53] proposed that the contribution to the electron density by an atom can be characterized by $n = \lambda\sqrt{K/V}$, where K and V are the bulk modulus and the atomic volume, respectively, and λ is a factor of unit value that takes care of the unit issues which is independent of the system. The applicability of the Miedema's model has been proved in many studies [26,54–56], it is therefore employed to analyze the abnormal behavior of the mentioned alloying elements above.

Accordingly, the characteristic electron density contributions for all the alloying elements were evaluated, and their values relative to that

of Ni, $\Delta n = n_X - n_{Ni}$ were deduced and shown in Fig. 2(c). One sees from Fig. 2(c) that Δn exhibits the same trend as that of k_G. What is more, it is found that most alloying elements have a lower characteristic electron density than Ni, while nearly all the elements exhibiting an abnormal behavior have a higher one than Ni. This suggests that the variation of the elastic constants is mainly dominated by the bonding strength, which is reflected by the characteristic electron density. Alloying elements that are prone to increase in the characteristic electron density will generally enhance the interatomic bonding, and consequently lead to an improvement in the elastic constants and moduli, i.e., a positive k_G.

3.3. Solid solution strengthening effects

Many models have been developed to quantify the SSS effects of the alloying element, among which some recent models [13–15], although yielding relatively accurate predictions by taking into account the interaction between the dislocation core and the solute explicitly, are however unsuitable for high throughput calculations due to the complicated workflow. The generally adopted Labusch model showing good agreement with experimental observations [57–61] was therefore adopted in this study to evaluate the strengthening effect quantitatively. Accordingly, the excess strength ($\Delta\sigma_{SSS}$) gained by SSS depends on the misfit factor (ε) and solute concentration (c) by

$$\Delta\sigma_{SSS} = 3Z \cdot G\varepsilon^{4/3}c^{2/3} \tag{4}$$

$$\varepsilon = \left[\left(\frac{\varepsilon_s}{1 + 0.5\,|\varepsilon_s|}\right)^2 + (\beta\,\varepsilon_b)^2\right]^{1/2} \tag{5}$$

where G is the shear modulus, Z is a constant dependent on the solvent, β is 16 for edge dislocation and 3 for screw dislocation. ε_b is the lattice misfit parameter defined by

$$\varepsilon_b = \frac{1}{a_0}\left(\frac{da}{dc}\right)_{c=0} \approx \frac{k_a}{a_0}, \tag{6}$$

and ε_s is the modulus misfit parameter given by

$$\varepsilon_s = \frac{1}{G_0}\left(\frac{dG}{dc}\right)_{c=0} \approx \frac{k_G}{G_0}. \tag{7}$$

The misfit factors for all the 35 alloying elements were evaluated accordingly and shown in Fig. 3(a). One sees again that the variation of ε also correlates with the group number. Elements in either end of the same period generally have higher strengthening abilities than those in the middle. Besides, the same trend is observed for both screw and edge dislocations, while in general the strengthening for edge dislocations would be more significant than that for the screw ones. Moreover, elements in the close vicinity of Ni within the same period, such as Cr, Mn, Fe, Co and Cu, exhibit rather small strengthening abilities, in that they do not differ much from Ni in either atomic size or electronegativity. While elements frequently found in Ni-based superalloys, such as Hf, Mo, Ti, W, Ta, etc., do have a large ε value, confirming their important role in strengthening the Ni-based superalloys. Nonetheless, Co and Cr are also frequently found in Ni-based superalloys yet their strengthening abilities are seen to be negligible, suggesting that their primary roles in the superalloys are not to strengthen the alloy.

To further isolate the contributions from the lattice misfit and the modulus misfit, the ratio of $\beta\,\varepsilon_b$ over ε is evaluated for each alloying element, which denotes the relative contribution of the lattice misfit to the strengthening ability. A value greater than $1/\sqrt{2}\approx0.71$ suggests that the lattice misfit dominates. One sees in Fig. 3(b) that a large scattering of data is observed. Nonetheless, for elements in the 2nd to the 4th period, it is the modulus misfit that dominates on average, as the ratios are generally lower than 0.71. While for elements in the 5th and 6th period, one sees that the ratios are mostly greater than 0.71, suggesting that the lattice misfit overwhelms. A roughly equal contribution is however found for Be, Mg, Mo, Hf, etc.; they also have a high total misfit factor ε, indicating that it is important for both the lattice misfit and the modulus misfit to be significant for effective strengthening. In general, the lattice misfit dominates for edge dislocations, while the modulus misfit overwhelms for screw dislocations.

3.4. Stability and energetics

The previous section revealed the ability of each alloying element to strengthen the Ni-based alloy, while for the strengthening to be effective, the resultant solid solution must be stable, in terms of both mechanics and thermodynamics. The mechanical or dynamical stability of a crystal can be assessed by the Born's criteria [62], which requires $C_{11} - |C_{12}| > 0$, $C_{11} + 2C_{12} > 0$ and $C_{44} > 0$ for cubic crystals. It is found that all the solid solution models examined in this work satisfied the Born's criteria, suggesting their dynamical stability. Besides, large B/G ratios (>1.75) were also found for all the models, indicating that they are intrinsically ductile according to the Pugh's criteria [63].

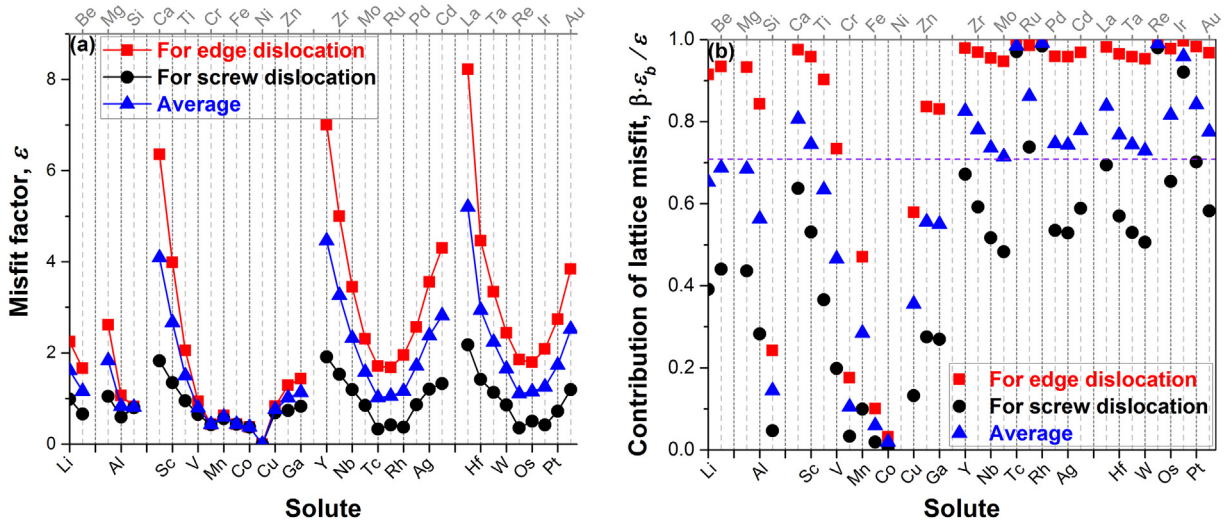

Fig. 3. The misfit factor (a) and the contribution of lattice misfit to the misfit factor (b) for Ni-based binary solid solutions in the order of atomic number of the solute.

To evaluate the thermodynamic stability, the solution enthalpy will be the quantity of relevance, which is defined as the energy change induced by replacing a matrix atom in an infinite crystal by a solute one [64]:

$$\Delta H_{\mathrm{sol}} \cong \Delta E_{\mathrm{sol}} = \lim_{n\to\infty}\left[E_{\mathrm{Ni}_{n-1}\mathrm{X}} - (n-1)E_{\mathrm{Ni}} - E_{\mathrm{X}}\right], \tag{8}$$

where $E_{\mathrm{Ni}_{n-1}\mathrm{X}}$, E_{Ni}, and E_{X} are the total energies for the substitutional solid solution $\mathrm{Ni}_{n-1}\mathrm{X}$, pure FCC Ni, and pure solute X in the FCC structure, respectively. In practice, it however can be evaluated by

$$\Delta H_{\mathrm{sol}} = \left(\frac{\partial \Delta H_{\mathrm{mix}}}{\partial c}\right)_{c=0}, \tag{9}$$

with the heat of mixing ΔH_{mix} given by

$$\Delta H_{\mathrm{mix}} = E_{\mathrm{Ni}_{1-c}\mathrm{X}_c} - (1-c)E_{\mathrm{Ni}} - c\cdot E_{\mathrm{X}} \tag{10}$$

At the dilute limit, we would expect

$$\Delta H_{\mathrm{mix}} \approx \Delta H_{\mathrm{sol}} \cdot c \tag{11}$$

For simplicity, we could therefore estimate the solution enthalpy by linear regression the heat of mixing calculated as a function of solute concentration. Fig. 4 shows the solution enthalpies for the 35 alloying elements in Ni thus evaluated. It is seen that the variation in ΔH_{sol} is relatively complicated, which should be attributed to the combination of size and electronic effects. For each period, it generally decreases in the beginning, increases later on, and then decreases again, with two peaks observed for the 4th to the 6th periods. Roughly half of the alloying elements show a negative solution enthalpy, while the other half a positive one. It is noticed that the solution enthalpies derived here agree well with the calculated substitutional energy by Chen et al [65], in terms of both the trend and the magnitude.

Generally speaking, a negative solution enthalpy indicates a reduction in the total enthalpy while forming the solid solution, and in turn a high propensity to form solid solutions. On the contrary, a positive solution enthalpy generally suggests low propensity to form solid solutions. [53,66] For example, both Ni–Ag and Ni–Au are known to be immiscible systems, their solution enthalpies are indeed positive, larger than 0.50 eV/atom. However, this does not rule out the possibility for elements with a positive solution enthalpy to form thermodynamically stable solid solutions with Ni, as the increase in entropy leverages the total free energy. Furthermore, there is also uncertainty in the evaluated solution enthalpy, roughly on the order of 0.05 eV/atom. Consequently, we can denote elements with a calculated solution enthalpy lower than 0.10 eV/atom as thermodynamically favorable, while those higher than 0.10 eV/atom as unlikely. Accordingly, Be, Mg, Al, Si, Sc, Ti, V, Cr, Mn, Fe, Co, Zn, Ga, Y, Zr, Nb, Mo, Rh, Hf, Ta, W, and Pt are thermodynamically favorable, while Li, Ca, Cu, Tc, Ru, Pd, Ag, Cd, La, Re, Os, Ir, and Au are marginal candidates to form solid solutions in Ni.

Although ΔH_{sol} indicates the propensity to form solid solutions, it however does not adequately characterize the solubility of an element, as the latter also depends on the thermodynamics of the coexisting/competing phase with the solid solution in the binary system. For example, Co has a negative ΔH_{sol} with Ni while the magnitude is small. They can form solid solutions throughout the composition range. The ΔH_{sol} for Ir in Ni is positive but with a small magnitude, a continuous solid solution is also found between them and Ni. While for Al, Si and Mg, although their ΔH_{sol} are negative and of large magnitude, the corresponding solubility is generally less than 20 at.%, because they tend to form intermetallic compounds with Ni. Consequently, the solubility of the alloying elements in Ni cannot be estimated merely from ΔH_{sol}.

The strengthening effect of an alloying element, as seen from Eq. (4), depends on both the misfit factor and the concentration of the alloying element. Besides, it also depends on the temperature. The Labusch model however does not take into account the temperature effect explicitly, a modification that reflects the variation of the critical resolved shear stress (ΔCRSS, τ) against temperature can be given as [61,67],

$$\tau = \Delta\sigma_{SSS}\, e^{-\mathrm{m}k_B T/W_0} \tag{12}$$

where k_B is the Boltzmann constant, $m = 25 \pm 2.3$, T is the absolute temperature and W_0 describes the binding energy of an edge-dislocation segment with the solute atoms in its proximity. According to Ref. [61, 67, 68], Eq. (12) is reliable within the low-temperature regime up to 1/3 of the absolute melting temperature, e.g. 573 K for Ni, and W_0 can be estimated to be 1.5×10^{-19} J.

As the solubility cannot be assessed directly from the solution enthalpy, the experimental saturate concentrations (c_m) of the alloying elements in FCC Ni at a typical working temperature for steam turbine of 573 K will be employed to quantify their respective "maximum strengthening effect", i.e., the strengthening potential. Accordingly, the extra strength contributed by the solid-solution strengthening, $\tau_{max} = \tau(c_m, T)$, at 573 K was evaluated and displayed in Fig. 5. One sees that by combining the strengthening ability and the solubility, the strengthening potential reveals a quite different trend for the alloying elements studied comparing to that of the misfit factor and/or the solution

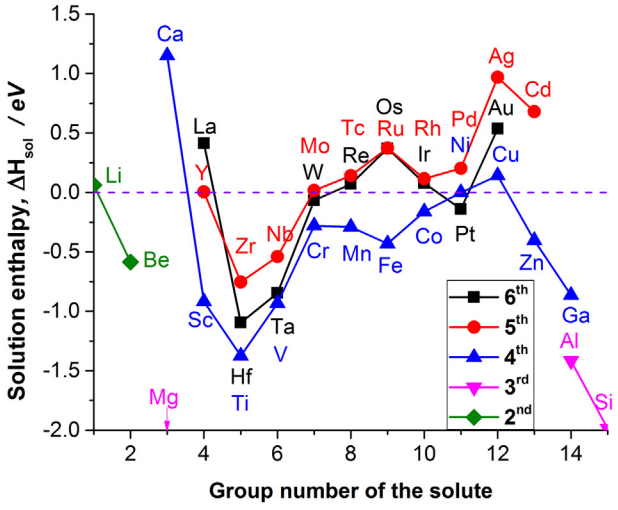

Fig. 4. Solution enthalpies for different elements in Ni-based solid solutions.

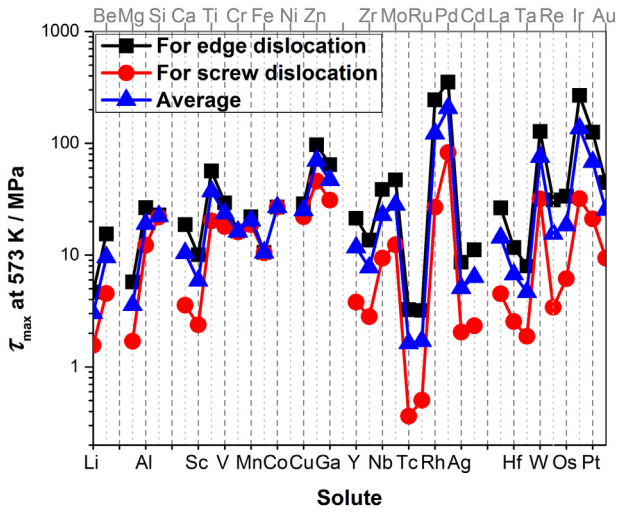

Fig. 5. Solid-solution strengthening potentials of the alloying elements in Ni-based solid solutions at 573 K.

enthalpy. Pronounced strengthening potentials are observed for elements like Zn, Rh, Pd, W, Ir, and Pt. Among them, some elements, such as Zn, W and Pt, gain their high strengthening potentials because of their high strengthening abilities, i.e., large misfit factors. Some elements, like Pd, Rh and Ir, achieve their high strengthening potentials due to their high solubility. While for elements like Ti and Mo, although their strengthening potentials are not that pronounced, their high strengthening abilities still warrant their wide application in Ni-based superalloys. Alloying elements such as Rh, Pd, and Ir, although having high strengthening potentials, they are however too scarce on earth, and are therefore less promising for strengthening the Ni-based superalloys.

Re worthies some additional attention. It has been seen that Re plays a rather crucial role in promoting the high temperature strength of Ni-based superalloys [2,69], one however notices in this work that it has both a small lattice misfit and a small modulus misfit with Ni, and in turn a low solid solution strengthening ability, as evidenced in Fig. 2. Besides, Re also has a positive solution enthalpy in Ni, although of small magnitude and comparable to that of Cu. However, its crystalline structure is HCP leading to a marginal solubility in Ni. As a result, its solid solution strengthening potential is essentially negligible. The crucial role it plays in Ni-based superalloys must take effects through other mechanisms.

3.5. Strengthening under high temperatures

For metals under high-temperature applications, creep is frequently of great concern. The creep rate ($\dot{\varepsilon}$) generally correlates with the stress applied and the diffusion processes [70,71], e.g.

$$\dot{\varepsilon} = AD_{\text{eff}}\left(\frac{\gamma_{\text{SFE}}}{Gb}\right)^3\left(\frac{\sigma-\sigma_b}{E}\right)^4 \tag{13}$$

where A is a materials dependent parameter, D_{eff} is the effective diffusion coefficient, γ_{SFE} is the stacking fault energies, σ_b is the back stress, b is the magnitude of the Burger's vector, E and G are the Young and Shear moduli, respectively. Strengthening would therefore be expected if the diffusion can be retarded. Besides, the stacking fault energy also plays a key role in the creep process. [2,6] A reduction in the stacking fault energy tends to expand the width between the partial dislocations, and in turn reduces the dislocation mobility. [70–73] Consequently, it is of necessity to examine the effect of solutes on the diffusion coefficient and the stacking fault energy if the strengthening effect under high temperatures is pursued.

In this regard, considerable investigations have been performed to examine the effect of alloying elements on the stacking fault energy and the diffusion coefficient of dilute Ni-based alloys. [18,28,74] It is found that those solutes with a relatively large size are prone to reduce the stacking fault energy [28], while the influence on the diffusion coefficient correlates with the bulk modulus rather than the atomic size [18]. Nonetheless, reports on the composition dependence are scarce because of the high computational demands. In this study, the influences of the alloying elements on the diffusion coefficients or the stacking fault energies will therefore not be calculated. Instead, the data reported in Ref. [18, 28, 74] would be adopted for some discussions.

The difference in diffusion coefficients for different solutes in many cases shows a larger order of magnitude than that of stacking fault energies according to the reported data, suggesting that the change in the diffusion coefficient is more significant than that in the stacking fault energy. For example, the change in stacking fault energy induced by Re is about 50% (from 114.40 mJ/m^2 to 60.79 mJ/m^2), while the change in diffusion coefficient is about 4 orders of magnitude (from 4.34×10^{-17} m^2/s to 7.78×10^{-21} m^2/s) at 1200 K [74]. This is because the alloying elements affect the diffusion coefficients mainly by modifying the diffusion energy barrier, which is generally on the same/similar order as that to the stacking fault energy. The diffusion coefficient depends however exponentially on the energy barrier, the influence of the alloying elements on the diffusion energy barrier will therefore dominate its effect on the high temperature performance of the alloys. Data reported in Ref. [18, 74] suggests that the addition of Re, Os, Ir, Tc, Ru, and Mo enhance the diffusion energy barrier effectively, and they would therefore be beneficial to improve the high temperature performance of the Ni alloys. Combining with the present results on strengthening ability and strengthening potential, as well as the influences on diffusion coefficients, it can be concluded that W and Mo might be promising alloying elements besides Re in warranting the high temperature performance of Ni. [2,18] As a tradeoff, parts serving at intermediate temperatures where the creep process is insignificant, elements with moderate to high misfit factors, and appreciable solubilities, e.g. V, Al, Ti, Ta, Pt, Rh, and Nb, would be good candidates to strengthen Ni. While to assess the comprehensive strengthening effects of the alloying elements at extremely high temperature, the de-mixing and precipitation of the solutes should be taken into account, which would correlate closely with the kinetic process and are beyond the topic of this work.

4. Conclusions

The composition-dependent lattice constants, elastic constants, shear modulus and energetics of 35 binary Ni-based solid solutions were calculated using high-throughput density functional theory calculations. The SSS effects of the alloying elements were evaluated by incorporating the Labusch model. The main conclusions are:

(1). The calculated lattice constants and shear moduli of the solid solution models are mostly seen to scale linearly with the composition, and the calculated data are in good accordance with the available experimental results.
(2). The variations of the lattice misfit and the modulus misfit are found to depend on the position of the alloying element in the periodic table. In general, the lattice misfit is dominated by the atomic size of the alloying element, while the modulus misfit shows an inverse trend as the lattice misfit. Most of the 2nd to 6th period metallic elements tend to dilate the lattice of Ni but to reduce the shear modulus.
(3). The strengthening ability incorporated both the lattice and modulus misfits reveals that elements in both ends of the same period tend to have higher strengthening ability than those in the middle. For metallic elements in the 2nd to the 4th period, it is the modulus misfit that overwhelms, while for those in the 5th to the 6th period the lattice misfit dominates the strengthening ability.
(4). Elements in the close vicinity of Ni within the same period, such as Cr, Mn, Co, Fe, and Cu, exhibit rather small strengthening ability, while elements frequently found in Ni-based superalloys, such as Hf, Mo, Ti, W, Ta, etc., do introduce appreciable misfit factors. Yet elements like Cr and Co are also frequently found in Ni-based superalloys, while their primary roles are not to provide solid solution strengthening.
(5). All the solid solution models are found to be dynamically stable and intrinsically ductile. While the solution enthalpies derived suggest that Be, Mg, Al, Si, Sc, Ti, V, Cr, Mn, Fe, Co, Zn, Ga, Y, Zr, Nb, Mo, Tc, Rh, Hf, Ta, W, Re, Ir, and Pt are thermodynamically favorable to form solid solutions with Ni, while Li, Ca, Cu, Tc, Ru, Pd, Ag, Cd, La, Re, Os, Ir, and Au are unlikely.
(6). The solution enthalpy however cannot be employed to assess the equilibrium solubility of the alloying elements. Instead, experimental solubilities at 573 K were used to evaluate the strengthening potentials of the alloying elements. Zn, Rh, Pd, W, Ir, and Pt are found to have high strengthening potentials because of the large strengthening ability and/or the large solubility.
(7). Re is critical for Ni-based superalloys, while its strengthening ability and solid solution propensity in Ni are however not prominent.

Data on diffusion reported by previous investigation revealed that it could enhance the diffusion energy barrier and in turn improve the high-temperature performance of the Ni-based superalloys.

(8). Tradeoff on the strengthening ability and solubility suggests that elements such as V, Ti, T, Pd, Rh, Nb, etc., could be promising candidates to provide SSS effects for Ni under low temperatures. While for high-temperature applications, elements like Re, Os, Ir, Tc, W, Ru, and Mo that tend to retard the diffusion in Ni are promising. Considering the abundance on earth and cost, Mo and W might be attractive.

Data availability

The data that support the findings of this study are available from the corresponding author upon reasonable request.

Declaration of Competing Interest

The authors declare that they have no known competing financial interests or personal relationships that could have appeared to influence the work reported in this paper.

Acknowledgement

This work is supported by the National Key R&D Program of China (2017YFB0701501), the National Natural Science Foundation of China (51620105012), and MaGIC of Shanghai Jiao Tong University. All the calculations were performed on the π 2.0 cluster at Shanghai Jiao Tong University. And the authors wish to thank Mr. Jie Wang for technical support on the supercomputers.

Appendix A. Supplementary data

Supplementary data to this article can be found online at https://doi.org/10.1016/j.matdes.2020.109359.

References

[1] R.C. Reed, The Superalloys: Fundamentals and Applications, Cambridge University Press, Cambridge, 2006 (372pp. ISBN 0-521-85904-2).
[2] E. Fleischmann, M.K. Miller, E. Affeldt, U. Glatzel, Quantitative experimental determination of the solid solution hardening potential of rhenium, tungsten and molybdenum in single-crystal nickel-based superalloys, Acta Mater. 87 (2015) 350–356.
[3] G.P.M. Leyson, W.A. Curtin, Friedel vs. Labusch: the strong/weak pinning transition in solute strengthened metals, Philos. Mag. 93 (2013) 2428–2444.
[4] R. Bullough, R.C. Newman, The kinetics of migration of point defects to dislocations, Rep. Prog. Phys. 33 (1970) 101–148.
[5] J.D. Eshelby, R.E. Peierls, The determination of the elastic field of an ellipsoidal inclusion, and related problems, Proc. R. Soc. Lond. Ser. A 241 (1957) 376–396.
[6] H. ur Rehman, K. Durst, S. Neumeier, A. Sato, R. Reed, M. Göken, On the temperature dependent strengthening of nickel by transition metal solutes, Acta Mater. 137 (2017) 54–63.
[7] J. Friedel, R. Smoluchowski, Les dislocations, Phys. Today 10 (7) (1957) 36–39.
[8] R.L. Fleisgher, Solution hardening, Acta Metall. 9 (1961) 996–1000.
[9] R.L. Fleischer, Substitutional solution hardening, Acta Metall. 11 (1963) 203–209.
[10] R. Labusch, Statistische theorien der mischkristallhärtung, Acta Metall. 20 (1972) 917–927.
[11] R. Labusch, Statistical theory of dislocation configurations in a random array of point obstacles, J. Appl. Phys. 48 (1977) 4550–4556.
[12] R.A. Labusch, A statistical theory of Solid solution hardening, Phys. Status Solidi 41 (2010) 659–669.
[13] G.P. Leyson, W.A. Curtin, L.G. Hector Jr., C.F. Woodward, Quantitative prediction of solute strengthening in aluminium alloys, Nat. Mater. 9 (2010) 750–755.
[14] G.P.M. Leyson, L.G. Hector, W.A. Curtin, Solute strengthening from first principles and application to aluminum alloys, Acta Mater. 60 (2012) 3873–3884.
[15] D. Ma, M. Friák, J.V. Pezold, D. Raabe, J. Neugebauer, Computationally efficient and quantitatively accurate multiscale simulation of solid-solution strengthening by ab initio calculation, Acta Mater. 85 (2015) 53–66.
[16] J.B. le Graverend, A. Jacques, J. Cormier, O. Ferry, T. Schenk, J. Mendez, Creep of a nickel-based single-crystal superalloy during very high-temperature jumps followed by synchrotron X-ray diffraction, Acta Mater. 84 (2015) 65–79.
[17] L. Dirand, J. Cormier, A. Jacques, J.P. Chateau-Cornu, T. Schenk, O. Ferry, P. Bastie, Measurement of the effective γ/γ' lattice mismatch during high temperature creep of Ni-based single crystal superalloy, Mater. Charact. 77 (2013) 32–46.
[18] C.Z. Hargather, S.L. Shang, Z.K. Liu, A comprehensive first-principles study of solute elements in dilute Ni alloys: diffusion coefficients and their implications to tailor creep rate, Acta Mater. 157 (2018) 126–141.
[19] L. Vegard, The constitution of mixed crystals and the space occupied by atoms, Z. Phys. 5 (1921) 17–26.
[20] K.A. Gschneidner Jr., G.H. Vineyard, Departures from Vegard's law, J. Appl. Phys. 33 (1962) 3444–3450.
[21] V.A. Lubarda, On the effective lattice parameter of binary alloys, Mech. Mater. 35 (2003) 53–68.
[22] Y. Wang, Z.K. Liu, L.Q. Chen, Thermodynamic properties of Al, Ni, NiAl, and Ni_3Al from first-principles calculations, Acta Mater. 52 (2004) 2665–2671.
[23] T. Wang, L.Q. Chen, Z.K. Liu, Lattice parameters and local lattice distortions in fcc-Ni solutions, Metall. Mater. Trans. A 38 (2007) 562–569.
[24] S.L. Shang, D.E. Kim, C.L. Zacherl, Y. Wang, Y. Du, Z.K. Liu, Effects of alloying elements and temperature on the elastic properties of dilute Ni-base superalloys from first-principles calculations, J. Appl. Phys. 112 (2012), 053515,
[25] D. Kim, S.L. Shang, Z.K. Liu, Effects of alloying elements on thermal expansions of γ-Ni and γ'-Ni_3Al by first-principles calculations, Acta Mater. 60 (2012) 1846–1856.
[26] D. Kim, S.L. Shang, Z.K. Liu, Effects of alloying elements on elastic properties of Ni by first-principles calculations, Comput. Mater. Sci. 47 (2009) 254–260.
[27] C.L. Zacherl, S.L. Shang, D.E. Kim, Y. Wang, Z.K. Liu, Effects of Alloying Elements on Elastic, Stacking Fault, and Diffusion Properties of Fcc Ni from First-Principles: Implications for Tailoring the Creep Rate of Ni-Base Superalloys, John Wiley & Sons, Inc., 2012
[28] S.L. Shang, C.L. Zacherl, H.Z. Fang, Y. Wang, Y. Du, Z.K. Liu, Effects of alloying element and temperature on the stacking fault energies of dilute Ni-base superalloys, J. Phys. Condens. Matter 24 (2012), 505403,
[29] V.A. Lubarda, Apparent elastic constants of cubic crystals and their pressure derivatives, Int. J. Non Linear Mech. 34 (1999) 5–11.
[30] C. Nyshadham, C. Oses, J.E. Hansen, I. Takeuchi, S. Curtarolo, G.L.W. Hart, A computational high-throughput search for new ternary superalloys, Acta Mater. 122 (2017) 438–447.
[31] Z. Deng, Z. Zhu, I.H. Chu, S.P. Ong, Data-driven first-principles methods for the study and design of alkali superionic conductors, Chem. Mater. 29 (2016) 281–288.
[32] J.E. Saal, S. Kirklin, M. Aykol, B. Meredig, C. Wolverton, Materials design and discovery with high-throughput density functional theory: the open quantum materials database (OQMD), JOM 65 (2013) 1501–1509.
[33] K. Mathew, J.H. Montoya, A. Faghaninia, S. Dwarakanath, M. Aykol, H. Tang, I.h. Chu, T. Smidt, B. Bocklund, M. Horton, J. Dagdelen, B. Wood, Z.K. Liu, J. Neaton, S.P. Ong, K. Persson, A. Jain, Atomate: A high-level interface to generate, execute, and analyze computational materials science workflows, Comput. Mater. Sci. 139 (2017) 140–152.
[34] F. Birch, Finite elastic strain of cubic crystals, Phys. Rev. 71 (1947) 809–824.
[35] R.W. Hill, The elastic behavior of a crystalline aggregate, Proc. Phys. Soc. 65 (2002) 349.
[36] G. Kresse, J. Furthmüller, Efficient iterative schemes for ab initio total-energy calculations using a plane-wave basis set, Phys. Rev. B Condens. Matter 54 (1996) 11169–11186.
[37] G. Kresse, J. Furthmüller, Efficiency of ab-initio total energy calculations for metals and semiconductors using a plane-wave basis set, Comput. Mater. Sci. 6 (1996) 15–50.
[38] G. Kresse, D. Joubert, From ultrasoft pseudopotentials to the projector augmented-wave method, Phys. Rev. B 59 (1999) 1758–1775.
[39] J.P. Perdew, K. Burke, M. Ernzerhof, Generalized gradient approximation made simple, Phys. Rev. Lett. 77 (1996) 3865–3868.
[40] M. Methfessel, A.T. Paxton, High-precision sampling for brillouin-zone integration in metals, Phys. Rev. B Condens. Matter 40 (1989) 3616–3621.
[41] A. van de Walle, P. Tiwary, M. de Jong, D.L. Olmsted, M. Asta, A. Dick, D. Shin, Y. Wang, L.Q. Chen, Z.K. Liu, Efficient stochastic generation of special quasirandom structures, Calphad 42 (2013) 13–18.
[42] A. van de Walle, M. Asta, G. Ceder, The alloy theoretic automated toolkit: a user guide, Calphad 26 (2002) 539–553.
[43] J. Bøttiger, N. Karpe, J.P. Krog, A.V. Ruban, Measured and calculated thermoelastic properties of supersaturated fcc Ni(Al) and Ni(Zr) solid solutions, J. Mater. Res. 13 (2011) 1717–1723.
[44] H.A. Moreen, R. Taggart, D.H. Polonis, A model for the prediction of lattice parameters of solid solutions, Metall. Trans. A. 2 (1971) 265–268.
[45] E.A. Zen, Correlation of chemical composition and physical properties of dolomite, Am. J. Sci. 254 (1956) 51–60.
[46] A.W. Lawson, On Simple Binary Solid Solutions, J. Chem. Phys. 15 (1947) 831–842.
[47] J.D. Eshelby, The Continuum Theory of Lattice Defects, in: F. Seitz, D. Turnbull (Eds.), Solid State Phys, Academic Press 1956, pp. 79–144.
[48] J. Friedel, LX. Deviations from Vegard's law, London, Edinburgh Dublin Philos, Mag. J. Sci. 46 (1955) 514–516.
[49] E.S. Sarkisov, Variation in the lattice constants of solid solutions with composition and Vegard's rule, Russ. J. Phys. Chem. 34 (1960) 202.
[50] G. Shao, P. Tsakiropoulos, Lattice parameters of TM(3d)-Al solid solutions, Mater. Sci. Eng. A 271 (1999) 286–290.
[51] V.A. Lubarda, On the effective lattice parameter of binary alloys, Mech. Mater. 35 (2003) 53–68.
[52] H. Pottebohm, G. Neite, E. Nembach, Elastic properties (the stiffness constants, the shear modulus and the dislocation line energy and tension) of Ni-Al solid solutions and of the Nimonic alloy PE16, Mater. Sci. Eng. 60 (1983) 189–194.

[53] A.R. Miedema, On the heat of formation of solid alloys. II, J. Less-Common Met. 46 (1976) 67–83.
[54] C. Li, P. Wu, Correlation of bulk modulus and the constituent element properties of binary intermetallic compounds, Chem. Mater. 13 (2001) 4642–4648.
[55] C. Li, Y.L. Chin, P. Wu, Correlation between bulk modulus of ternary intermetallic compounds and atomic properties of their constituent elements, Intermetallics 12 (2004) 103–109.
[56] S.B. Ramos, N.V. González Lemus, G.F. Cabeza, A. Fernández Guillermet, Cohesive properties of (Cu,Ni)-(In,Sn) intermetallics: database, electron-density correlations and interpretation of bonding trends, J. Phys. Chem. Solids 93 (2016) 40–51.
[57] L. Čižek, P. Kratochvíl, B. Smola, Solid solution hardening of copper crystals, J. Mater. Sci. 9 (1974) 1517–1520.
[58] C.H. Cáceres, D.M. Rovera, Solid solution strengthening in concentrated Mg–Al alloys, J. Light. Met. 1 (2001) 151–156.
[59] J. Zander, R. Sandström, L. Vitos, Modelling mechanical properties for non-hardenable aluminium alloys, Comput. Mater. Sci. 41 (2007) 86–95.
[60] C. Pöhl, J. Schatte, H. Leitner, Solid solution hardening of molybdenum–hafnium alloys: Experiments and Modeling, Mater. Sci. Eng. A 559 (2013) 643–650.
[61] I. Toda-Caraballo, P.E.J. Rivera-Díaz-del-Castillo, Modelling solid solution hardening in high entropy alloys, Acta Mater. 85 (2015) 14–23.
[62] A.J.C. Wilson, Dynamical theory of crystal lattices by M. Born and K. Huang, Acta Crystallogr. 26 (2010) 702.
[63] S.F. Pugh, XCII. Relations between the elastic moduli and the plastic properties of polycrystalline pure metals, Philos. Mag. 45 (1954) 823–843.
[64] M.H.F. Sluiter, Y. Kawazoe, Prediction of solution enthalpies of substitutional impurities in aluminium, Model. Simul. Mater. Sci. Eng. 8 (2000) 221–232.
[65] W. Chen, W. Xing, H. Ma, X. Ding, X.Q. Chen, D. Li, Y. Li, Comprehensive first-principles study of transition-metal substitution in the γ phase of nickel-based superalloys, Calphad 61 (2018) 41–49.
[66] A.R. Miedema, R. Boom, F.R. De Boer, On the heat of formation of solid alloys, J. Less-Common Met. 41 (1975) 283–298.
[67] M.Z. Butt, Investigation of the activation-parameters of low-temperature slip in cubic metals, Czechoslov. J. Phys. 49 (1999) 1177–1184.
[68] M.Z. Butt, I.M. Ghauri, Effect of short-range order on the temperature dependence of plastic flow in α-brasses, Phys. Status Solidi A 107 (1988) 187–195.
[69] X. Zhang, H. Deng, S. Xiao, X. Li, W. Hu, Atomistic simulations of solid solution strengthening in Ni-based superalloy, Comput. Mater. Sci. 68 (2013) 132–137.
[70] Z. Guo, A.P. Miodownik, N. Saunders, J.P. Schillé, Influence of stacking-fault energy on high temperature creep of alpha titanium alloys, Scr. Mater. 54 (2006) 2175–2178.
[71] Z.L. Guo, N. Saunders, A.P. Miodownik, J.P. Schille, Quantification of high temperature strength of nickel-based superalloys, Mater. Sci. Forum 546-549 (2007) 1319–1326.
[72] F.A. Mohamed, T.G. Langdon, The transition from dislocation climb to viscous glide in creep of solid solution alloys, Acta Metall. 22 (1974) 779–788.
[73] B. Burton, The influence of stacking fault energy on creep, Acta Metall. 30 (1982) 905–910.
[74] C.Z. Hargather, S.L. Shang, Z.K. Liu, Data set for diffusion coefficients and relative creep rate ratios of 26 dilute Ni-X alloy systems from first-principles calculations, Data Brief 20 (2018) 1537–1551.